DIELECTRIC MEASUREMENT FOR SOLID CYLINDRICAL SAMPLES

N. Seleznev, A. Boyd, T. Habashy, C. Straley
Schlumberger-Doll Research, Ridgefield, US
S. Luthi, Delft University of Technology, The Netherlands

This paper was prepared for presentation at the International Symposium of the Society of Core Analysts held in Abu Dhabi, UAE, 5-9 October, 2004

ABSTRACT

In this paper we describe a coaxial-circular cell for wide band dielectric measurements on solid cylindrical samples. Combined with existing data-processing algorithms, the technique can be applied to a variety of materials including oilfield rocks. The simple cylindrical sample geometry is a distinctive feature of this method and is a significant advantage of the technique. Commonly used coaxial cells require cylindrical samples modified with a central hole to accommodate the inner electrode of the coaxial line. Although this configuration presents no problem for liquid samples, for solid samples, precise machining is required to insure good measurements. For rock materials, which must be ground into shape using circular diamond cutters, creating good coaxial samples for coaxial cells is an art; it can be difficult, or impossible, in case of weakly consolidated rocks. In addition, in a coaxial sample it is difficult to achieve homogeneous partial saturation. In contrast partial saturation of solid cylindrical samples can be achieved relatively easy. Hence the capability to measure simple cylindrical samples that this new cell provides not only simplifies the sample preparation but also allows for the partial saturation experiments.

We discuss the experimental set up, forward model and the inversion methodology, which are required for this geometry. We also assess the uncertainty associated with the measurement. The forward model was validated by the numerical modeling of the cell response. We obtained a good fit between measured and expected results for several materials with known permittivity and conductivity including brines and glycerol. Permittivity and conductivity of brines were calculated from the measurements of DC conductivity and temperature using the Klein-Swift model [3]. Glycerol permittivity was taken from Buckley and Maryott [4]. Measurements of carbonate rocks at partial saturations are presented.

INTRODUCTION

The knowledge of the permittivity and its frequency behavior is important in both basic and applied research. Dielectric measurements are a particularly informative technique for geophysical applications [1]. In the laboratory dielectric properties can be measured by different methods employing various sample sizes and shapes [5]. Until now coaxial cells were commonly utilized [5-8]. The knowledge of both reflection and transmission coefficients allows for closed form expression derivation and simplifies the computation

of permittivity and conductivity from experimental data. However these cells require a coaxial sample. In some cases, creating a coaxial sample is easy, as with a liquid sample. In other cases the inabilility to precisely shape the sample can limit the use of a coaxial cell. In case of weakly consolidated materials it is difficult to machine such a sample. This is especially true for rock materials which must be ground into shape rather than using more conventional machining methods. In addition to performing dielectric measurements, we would like to do other partial saturation measurements such as low frequency resistivity and NMR.
The coaxial geometry is not suitable for partial saturation experiments in the case of porous samples and the ancillary measurements require cylindrical samples.

Recently a new type of cell had been introduced [2]. This coaxial-circular cell uses cylindrically shaped samples and avoids the disadvantages of the common coaxial cell. It consists of two coaxial waveguides connected through to a central cylindrical section. In other words, the coaxial waveguides are abruptly truncated at the faces of the sample, which resides in a central cylindrical section and makes an electrical contact with the central electrodes of coaxial waveguides. The sample has a simple cylindrical geometry. We adopted this concept and made a cell for 3.81 cm (1.5 inch) diameter cores. We will refer to our cell as a cylindrical cell or a cylindrical dielectric cell.

FORWARD MODEL AND INVERSION METHODOLOGY:

We utilized a full wave model developed by Habashy [2]. The forward model approximates conical coaxial electrodes as coaxial electrodes of constant radius. The validity of this approximation was verified by a numerical modeling. We created a model with the exact dimensions of the cell and computed the response of a hypothetical sample. The modeled sample had permittivity of 80 and conductivity of 0.1 S/m at all frequencies. This sample was meant to resemble cell response to 0.1 S/m brine. The comparison between the forward model (assuming coaxial electrodes with a constant radius) and the numerical modeling with actual cell dimensions is presented in Fig. 2. The agreement between numerical results and the forward model validates our modeling of the conical electrodes as if they were of constant radius.

Determination of permittivity and conductivity of a sample from measured S parameters requires an inversion approach. We utilized an inversion methodology developed by Habashy [2] and based on a Gauss-Newton minimization algorithm.

The cost function was defined as the difference between the measured and the predicted responses weighted in proportion to the measurement confidence:

$$C(\bar{x}) = \sum_{i=1}^{M} W_i \cdot (S_i(\bar{x}) - m_i)^2 \qquad (1)$$

"M" is the number of measurements (in our case there are four complex S parameters and M=8), m_j is the observed response (measured data) and S_j is the corresponding

simulated response as predicted by the vector of model parameters, $\bar{x}$, $\bar{x} = [x_1 ... x_N]$, where "N" is the number of unknowns (N=2, corresponding to conductivity and dielectric constant). W_i is the measure of the confidence in m_j.

The inversion had been constrained by a non-linear transformation. If $x_{\max}$ is an upper bound on the model parameter x and $x_{\min}$ is a lower bound, then in order to ensure that $x_{\min} < x < x_{\max}$ at all iterations, we introduce the following transformation,

$$x = x_{\min} + \frac{x_{\max} - x_{\min}}{c^2 + 1} c^2, \qquad -\infty < c < +\infty \tag{2}$$

It is clear that

$$x \to x_{\min}, \quad \text{as } c \to 0$$
$$x \to x_{\max}, \quad \text{as } c \to \pm\infty \tag{3}$$

A Newton minimization approach is based on a local quadratic model of the cost function. The quadratic model is formed by taking the first three terms of the Taylor-series expansion of the cost function around the current k-th iteration $(\bar{x}_k)$, as follows,

$$C(\bar{x}_k + \bar{p}_k) \approx C(\bar{x}_k) + \bar{g}^T(\bar{x}_k) \cdot \bar{p}_k + \frac{1}{2} \bar{p}_k^T \cdot \bar{\bar{G}}(\bar{x}_k) \cdot \bar{p}_k, \tag{4}$$

where the subscript T indicates transposition and $\bar{p}_k = \bar{x}_{k+1} - \bar{x}_k$ is the step in $\bar{x}_k$ towards the minimum of the cost function $C(\bar{x})$. The vector $\bar{g}(\bar{x}) = \nabla C(\bar{x})$ is the gradient vector of the cost function $C(\bar{x})$ and $\bar{\bar{G}}(\bar{x}) = \nabla\nabla C(\bar{x})$ is the Hessian of the cost function $C(\bar{x})$. For the reconstruction of the conductivity and permittivity we utilized a variation of the Newton approach known as the Gauss-Newton algorithm. In the Gauss-Newton method, one discards the second order derivatives to avoid the expensive computation. The Gauss-Newton minimization approach has a rate of convergence that is slightly less than quadratic but significantly better than linear. It provides quadratic convergence in the neighborhood of the minimum.

The iteration process stops if the difference between two successive iterates, $(k+1)$-th and k-th, of the model parameters are within a prescribed tolerance factor, *tole*, of the cost function at the current iterate:

$$\left| C(\bar{x}_{k+1}) - C(\bar{x}_k) \right| \le tole \times C(\bar{x}_{k+1}) \tag{5}$$

The completion of the inversion process is achieved at cost function minimum. There are only two model parameters (sample permittivity and conductivity). It allows for a graphical representation of the cost function dependence on these parameters. In Fig. 3 the cost function magnitude at 10 MHz is plotted against the vertical axis. The permittivity and conductivity span in the horizontal plane. The map was calculated for a reflection measurement. True sample permittivity is 50 and conductivity is 0.3 S/m.

There is a single minimum of the cost function at ε =50 and σ=0.3 S/m. Hence at 10 MHz the choice of an initial vector of model parameters (initial guess) should not influence the result of inversion. The cost function behavior differs significantly at high frequencies. Fig. 4 displays analogous map at 2 GHz. Besides the correct minimum at ε =50 and σ=0.3 S/m there are several false minima. If the initial guess of the model parameters has been chosen sufficiently far from the true values of permittivity and conductivity the inversion process will likely be trapped in one of the false minima. In order to safeguard against this problem we utilize the knowledge of conductivity and permittivity at lower frequencies. For every next $(k+1)$-th measurement we set the initial guess to the values achieved at the previous (lower frequency) k-th step. Dielectric permittivity and conductivity are continuous functions of frequency and with sufficiently close spacing between subsequent measurements this algorithm provides a reliable reconstruction of model parameters.

EXPERIMENTAL SETUP AND PROCEDURE

A photograph of the experimental apparatus is shown in Fig. 1. The coaxial-circular cell is connected with a standard 7 mm coaxial cable to an Agilent 8753 ES Network Analyzer. The cell is made of stainless steel. The sample is located in a circular section sandwiched between two tapered coaxial electrodes. The coaxial electrodes are tapered so as to act as an adapter between the network analyzer's coaxial cable and the circular sample holder of the cell. The sample is in electrical contact with the center conductors of the coaxial sections of the cell which press against the sample's two flat ends. The diameter of the sample holder is 3.81 cm, the center conductor of the coaxial section has a diameter of 1.17 cm. The space between the center and outer conductors of the coaxial section is filled with Teflon. The characteristic impedance of the coaxial section is 50 Ohms. The cell was designed to make higher order TM modes reflected from the coaxial-circular junctions evanescent. The coaxial sections are sufficiently long to suppress these modes up to the highest frequency in our experiments.

The scattering parameters (S-parameters) across the cell terminals are measured by the network analyzer. The data acquisition is automated and controlled by a LabView application. All four S-parameters are recorded in the form of an amplitude (in dB) and phase (in degrees). The network analyzer is calibrated with a conventional full two-port calibration set. This set includes a short, an open and a load standards. This calibration establishes the plane of measurements at the connection between the analyzer's coaxial cables and the cell terminals.

Although the conventional calibration is effective in removing systematic analyzer and cable errors, imperfections in manufacturing process affect the cell response; the conical end pieces may not respond exactly like 50 Ohm coaxial line. In order to correct for these imperfections, several additional procedures have been utilized. One possibility is to move the plane of calibration to the faces of the cell’s coaxial elements, which could be achieved by calibrating the network analyzer at the end of the cell coaxial sections. This

approach has the advantage of providing complete error correction but requires new calibration standards to be made; a standard Hewlett-Packard calibration set cannot be connected to the open face of the coaxial section. We found it difficult to make standards with the required response due to various reasons including non-reproducible connections and eventually abandoned the effort.

Another way to enhance the accuracy of measurements is to remove the influence of the cones after the measurement. This could be done if the S matrix of each cone is known. The S matrix consists of four complex numbers describing an object's ability to transmit and reflect electromagnetic waves. Due to the symmetry of this matrix one has to define three independent complex scattering parameters. The limiting factor for this correction is the accuracy to which the S matrix can be determined. We have made three reflection measurements from different objects with known reflection response for each conical coaxial end piece. These three measurements can provide sufficient information to determine the S matrix when the reflecting objects have sufficiently different responses. An ideal set would include an open, a short and a perfect termination (50 Ohm load) but that set would leads us back to the problem of manufacturing good calibration standards for a non-standard connection. An alternative method that avoids the connection problem is to use liquids with known properties as reflection standards. We could not identify three liquids with sufficiently different scattering properties that a reliable S matrix determination could be made for the entire frequency range.

In the end, we used a simple normalization. A correction based on a single measurement of a known standard has been successfully used previously [2]. In that case the data was normalized with the measurement from an empty cell. We found we get more reliable results when the measurement is normalized to a material of uniform properties, which are similar to those of the sample to be tested.

We also assessed the uncertainty associated with the measurement. Sample permittivity and conductivity can be estimated from each of the four measured complex S-parameters. The inversion of these four values can yield four slightly different pairs of conductivity and permittivity values due to the inhomogeneity of the rock sample. The goal is to combine these values in such a way that the uncertainty will be minimized.

The accuracy of the amplitude and the phase measurements is limited to the accuracy of the network analyzer. For our experimental set up we estimated that the amplitude is known to within ± 0.3 dB, and the phase angle within $\pm 0.5^0$. Let subscript "k" denote values obtained from inversion of k-th S-parameter. These values consist of the real part of dielectric constant ε'_k and the complex part ε''_k. We compute the change in the dielectric constant alternately varying the phase and the amplitude of the k-th S-parameter within the accuracy of the measurement [10]. Corresponded change in the value of ε'_k is marked as $\Delta\varepsilon'_{kj}$ (j=1,2 for permittivity and conductivity).

Let

$$w'_k = 1 \Big/ \left(\sum_{j=1}^{2} (\Delta\varepsilon'_{kj})^2\right) \quad (6)$$

The combined estimate of ε' from four S-parameters is then obtained by taking a weighted average of ε_k with the weight factor w'_k

$$\bar{\varepsilon}' = \sum_i w'_k \varepsilon'_k \Big/ \sum_i w'_k \quad (7)$$

The uncertainty $\Delta\bar{\varepsilon}'$ associated with the $\bar{\varepsilon}'$ is found using the expression

$$\Delta\bar{\varepsilon}' = \sum_i w_k{}'^{1/2} \Big/ \sum_i w'_k \quad (8)$$

A similar procedure is applied to the imaginary part ε''.

RESULTS

The accuracy of our measurement has been verified on fluids with known dielectric properties: brines and glycerol. Brine dielectric constant and conductivity in a wide frequency band can be predicted with the Klein-Swift model. The required inputs are the DC brine conductivity and temperature. Comparison between experimentally obtained permittivity and conductivity of 10 Ohmm brine and Klein-Swift model prediction is shown in Fig. 5. Error bars are suppressed for clarity. Generally there is a good agreement between the measurement and the model. Around 1 GHz there is a slight discrepancy between inverted and modeled results. These discrepancies correspond to the propagation of the low order modes through the cylindrical waveguide. For oilfield rocks the dielectric constant does not reach sufficiently high values around 1 GHz to allow mode propagation and the measurement results are not affected.

The dielectric constant of brines doe not change significantly in the experimental frequency range. Also at 1 GHz, brines exhibit notably higher permittivity than saturated cores. Another set of measurements was made on pure organic liquids such as glycerol and 1,3 propanediol. Glycerol permittivity dispersion resembles the behavior of brine-saturated rocks. The measured permittivity and conductivity are shown **i**n Fig. 6. The obtained values are close to the ones reported in [4]. The uncertainty in the permittivity measurement is getting larger with decreasing frequency. This happens due to the fact that the sample size is becoming smaller compare to a wavelength causing the decrease in sensitivity to the sample characteristics. The magnitude of the uncertainty at a given frequency is mostly dependent on the sample conductivity and increases with increasing conductivity.

Measurement on a cylindrical limestone core fully saturated with oil is shown on the Fig. 7. This sample has 29% porosity. As it is expected there is no frequency dependence of permittivity. If the porosity is known then the matrix permittivity can be calculated from the measurement of a dry (or oil saturated) sample. This is an important capability for geophysical applications.

Finally, the results of our measurements on partially saturated limestone are presented on the Fig. 9. The dielectric permittivity and conductivity of the rock decreases with decreasing brine saturation. The ability to make measurements at partial saturations allow for a comparative analysis of mixing laws at selected frequencies. Such an analysis for carbonate rocks has been carried out [9].

CONCLUSION

We have described a cylindrical cell for a measurement of dielectric permittivity and conductivity over a wide frequency range. The cell has a conically shaped coaxial transition between network analyzer cables and coaxial-circular junction at the face of the sample. The conical end pieces are necessary in order to accommodate samples larger than the diameter of cable connections. Good agreement between the forward model predictions and the numerical modeling calculations validates the forward model and justifies the treatment of the conical-coaxial sections as coaxial cylinders, which were incorporated in the forward model.

The dielectric permittivity and conductivity of the sample are obtained from an inversion of measured S-parameters. The inversion is based on a Gauss-Newton minimization with a variable initial guess. This methodology allows for a fast and reliable reconstruction of the permittivity and conductivity from the measured data.

Measurement uncertainties have been estimated and error bars are computed based on sensitivity of complex dielectric constant to the variation in S-parameters.

Finally, we have established good agreement between measured and expected values of dielectric permittivity and conductivity for 10 Ohmm brine. RF properties of the salt solution were derived from the DC measurements of temperature and conductivity based on Klein-Swift model.

ACKNOWLEDGEMENT

The authors would like to thank Matthieu Simon for carrying out numerical simulations, Jean-Baptist Clavaud for developing a Labview application, Abby Matteson, Wave Smith and Phillip Frulla for preparing rock samples.

REFERENCES

1. Calvert, T.J., Rau N.R., “Electromagnetic propagation… A new dimension in logging”, SPE 6542.
2. Habashy, T., Taherian R., Yuen J., Kong J., 1991. “A coaxial-circular waveguide for dielectric measurement”, IEEE Trans. Geoscience and Remote Sensing, vol.29, No.2, 321-330

3. Klein, L., and Swift, T., 1977. “An improved model for the dielectric constant of sea water at microwave frequencies”, IEEE Trans. On Antennas and Propagation, vol. AP-25, No.1, 104-111
4. Buckley F., and Maryott A., “Tables of dielectric dispersion: data for pure liquids and dilute solutions”, National Bureau of Standards Circular 589, November 1, 1958.
5. H.E. Bussey, “Measurement of RF properties of materials. A survey,” Proc. IEEE, vol.55, pp.1046-1053, 1967.
6. L.C. Shen, A laboratory technique for measuring dielectric properties of core samples at ultra high frequencies”, SPE 12552, 1983
7. W.B. Weir, “Automatic measurement of complex dielectric constant and permeability at microwave frequencies”, Proc, IEEE, vol. 62, no.1, pp.33-36, 1974
8. R.N. Rau. And R.P. Wharton, “Measurement of core electrical parameters at UHF and microwave frequencies”, SPE 9380, 55th annual meeting of the SPE, Dallas, Texas, Sept. 21-24, 1980
9. Seleznev, N., Boyd, A., Habashy, T., Luthi, S., “Dielectric mixing laws for fully and partially saturated carbonate rocks”, Proceedings of the SPWLA 45th Annual Logging Symposium, June 6–9, 2004, The Netherlands
10. Banavar, J.R., Sen, P.N., Tomanic, J., Wong, P., “Inversion method for obtaining dielectric data from scattering parameters”, Schlumberger internal report.

Fig. 1. Cylindrical dielectric cell connected to a network analyzer.

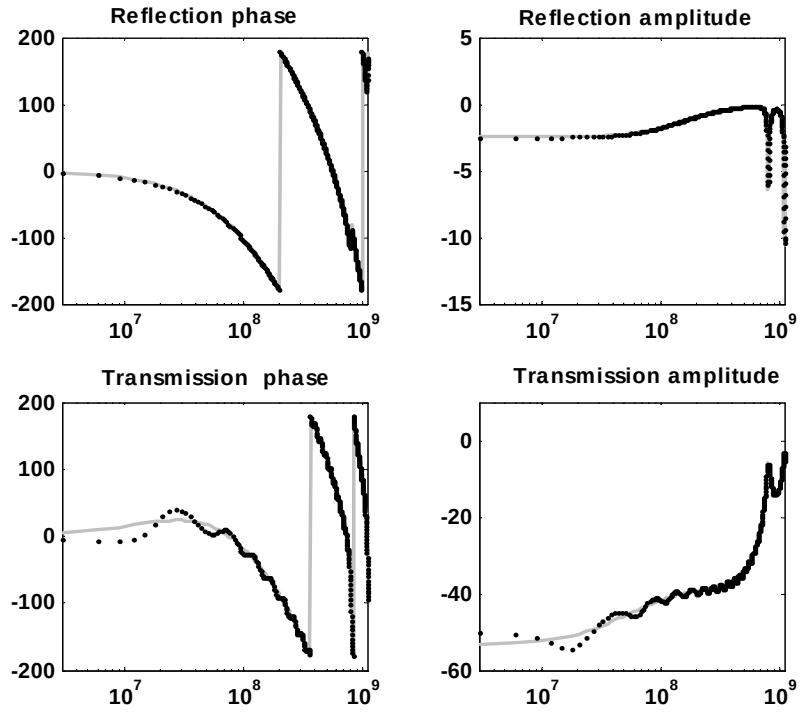

Fig.2. Comparison between numerical simulations of the cell response (dots) and the forward model (solid lines). Sample permittivity is 80 and conductivity is 0.1 S/m.

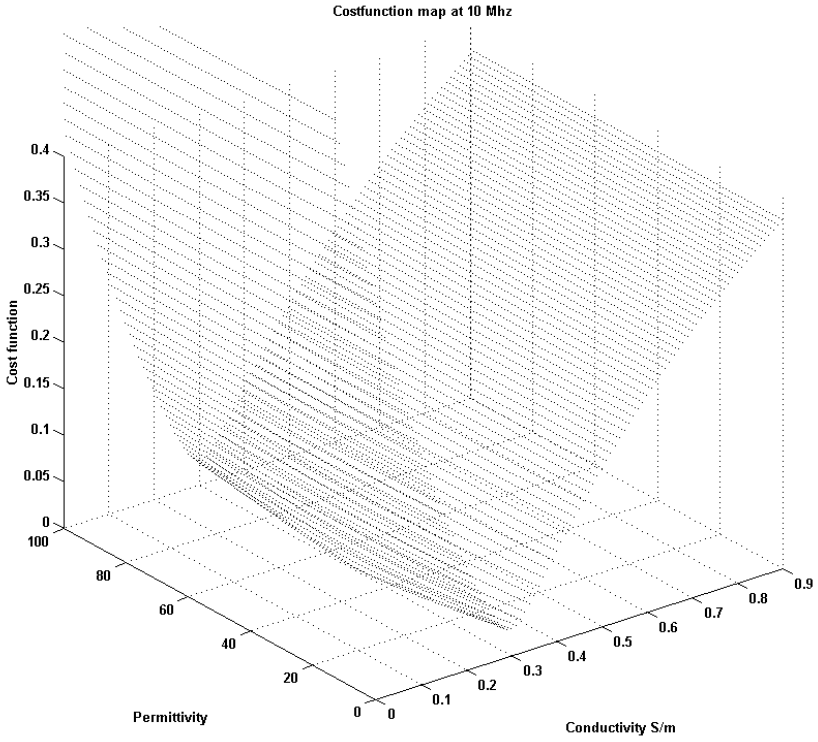

Fig. 3. Cost function map at 10 MHz

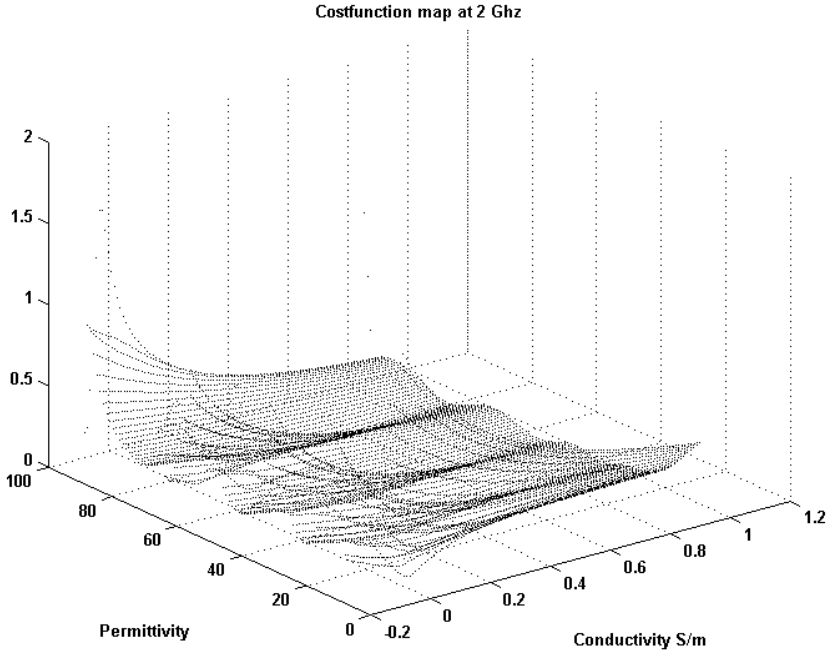

Fig. 4 Cost function map at 2 GHz

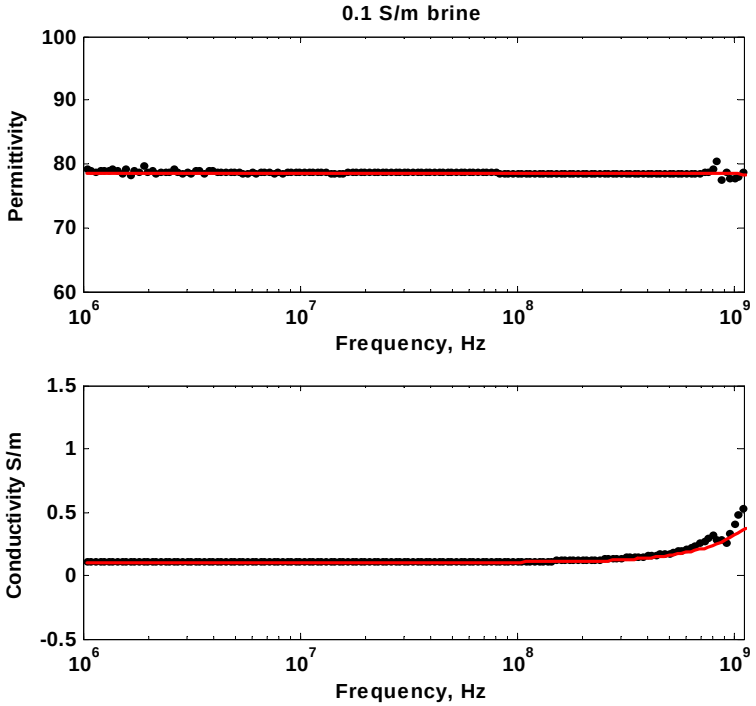

Fig. 5. Measured (black) permittivity and conductivity of a 0.1 S/m brine versus Klein-Swift model (red).

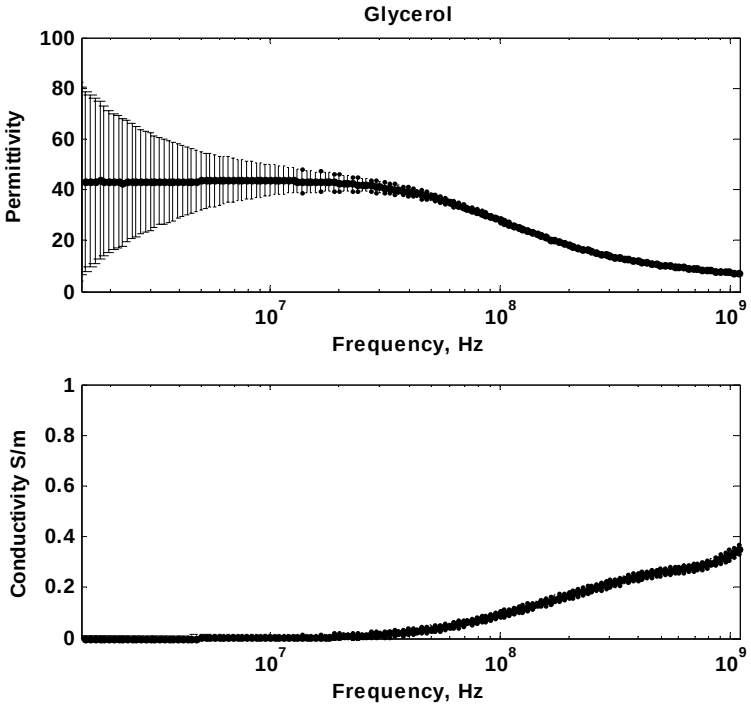

Fig. 6. Permittivity and conductivity of a pure glycerol.

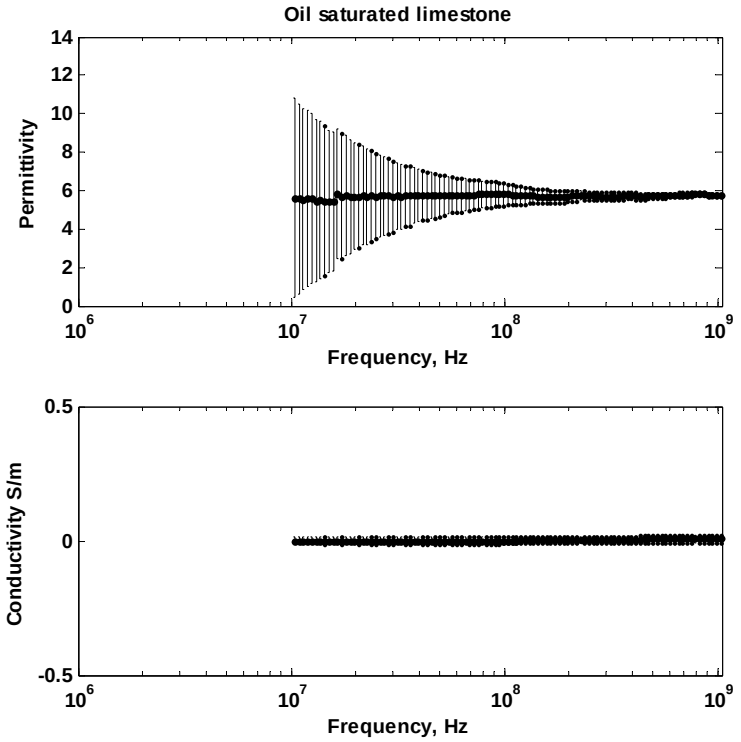

Fig. 7. Limestone fully saturated with oil. Porosity is 29 pu.

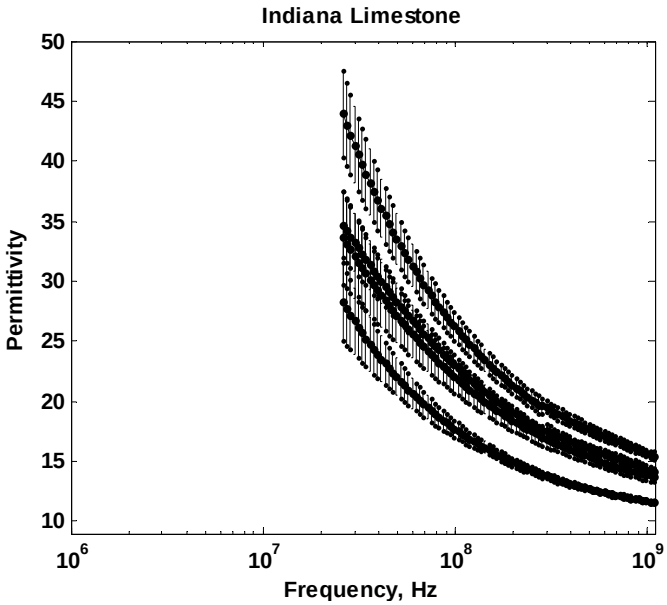

Fig. 8. Limestone at four different partial saturations. Water saturation decreases with decreasing dielectric constant.